Proceedings of the Seventh Arab Structural Engineering Conference
24 - 26 November 1997 Kuwait

THEORETICAL ASSESSMENT OF FRP REPAIRED REINFORCED CONCRETE STRUCTURES

Ibrahim M. Ibrahim
Professor and Vice Dean for Graduate Studies

Ibrahim G. Shaaban
Asst. Professor

Wael Abo Elmagd
Graduate Student

Department of Civil Engineering, Faculty of Engineering, Shoubra, Cairo, Egypt

ABSTRACT

The development of a static material nonlinear finite element computer program for the analysis of reinforced concrete (R.C) slabs and shells retrofitted with fiber reinforced plastics (FRP) is presented herein. The proposed material model for reinforced concrete section attached with FRP is based on the layered approach. The concrete model takes the elastoplastic behavior in compression domain, and the elastic brittle fracture behavior in tension domain, into consideration, as well as compression softening, crack tension stiffening, and rotating crack concept. The steel is modeled by an idealized bilinear curve identical in both tension and compression. The FRP is treated as an orthotropic layer with elastic brittle fracture behavior. The developed formulations and software show an excellent agreement with the experimental and numerical results in the literature.

INTRODUCTION

Since the beginning of R.C type of construction, designers have always been concerned with the corrosion of steel reinforcement particularly in structures located in aggressive environments such as coastal and marine structures. Corrosion progresses rapidly in salt-contaminated concrete, resulting in cracking and spalling of the concrete section [1]. Strengthening and repair of damaged structural elements is essential and preferable than replacing these elements in some special cases for their historical values, such as in old and monumental palaces, or for their strategical locations, such as in very heavy traffic bridges.

The use of FRP composites for a variety of industrial applications has been rapidly increasing in the recent years. The main reasons for using these types of materials are their superior strength-to-weight ratio, and durability in corrosive environments, as compared with conventional materials [2]. In addition to the superior strength properties, many composites have shows much better fatigue performance than structural metals. The first recorded application of FRP composites, was in the air-craft industry dated as far back as 1944 [3]. Although fiber reinforced plastics (FRP) are now widely used in a range of structural applications, they are still rarely used in strengthening concrete structures [4]. This may be attributed to the complexities arising from the nature and structure of these composite sections, and the unknown behavior of composite section made of FRP attached to R.C. which affect their analysis and design procedures [5]. In addition, the repair of concrete structures using FRP composites is costly compared with the strengthening by the conventional materials. Therefore, accurate methods for analysis and design of R.C elements strengthened by FRP are essential in order to optimize the use of FRP material in the repair work, or in other words reducing the cost of repair by advanced composite materials.

The main objective of this investigation is to predict the behavior of reinforced concrete section rehabilitated by FRP sheets accurately. In order to achieve this aim, a static material nonlinear finite element computer program based on isoparametric 4-nodes layered element formulation was developed. The composite section made of reinforced concrete and FRP is modeled properly using the layered approach. In this approach, the proposed section is divided up through the thickness into a number of layers. Each layer is assumed to be in a state of plane stress. Each of the proposed material models is then applied to each layer individually. In the following section, the constitutive models will be briefly summarized. The formulation of these models is detailed elsewhere [4].

MATERIAL MODELING

In the nonlinear analysis of reinforced concrete members strengthened by FRP, the section can be divided into a number of concrete layers through the thickness, while the steel reinforcement and FRP are smeared into equivalent steel and FRP layers, and each layer is assumed to be in a state of plane stress. The concrete layer model contains the elastoplastic behavior in compression, elastic brittle fracture behavior in tension, crack tension stiffening, compression softening, and rotating crack concept [6]. The steel reinforcement layer is modeled by an idealized bilinear curve identical in both tension and compression [7]. The FRP layer is treated as an orthotropic layer with elastic brittle fracture behavior [5]. These material models have been tested against experimental data and good agreement was found [6,7].

Concrete Layers

In this investigation, the theory of plasticity is employed to describe the strain hardening behavior of plain concrete [6]. The initial and subsequent yield surfaces assumed for the concrete (see Fig.1) can be defined by the same yield function expressed in the following form;

$$f(\{\sigma\}, \sigma) = F(\{\sigma\}) - \sigma = 0 \qquad (1)$$

where, $\{\sigma\} = \{\sigma_x, \sigma_y, \tau_{xy}\}$ is the stress vector.

The function F can be looked upon as a loading function and σ is a hardening parameter called "the equivalent stress"[7]. The detailed definitions of the various failure surfaces can be obtained from [6 and 7].

The constitutive matrices for elastic concrete, singly cracked concrete, and doubly cracked concrete, respectively, are:

$$[C]_c = \frac{E_c}{(1-\nu^2)}\begin{bmatrix} 1 & \nu & 0 \\ \nu & 1 & 0 \\ 0 & 0 & (1-\nu)/2 \end{bmatrix},$$

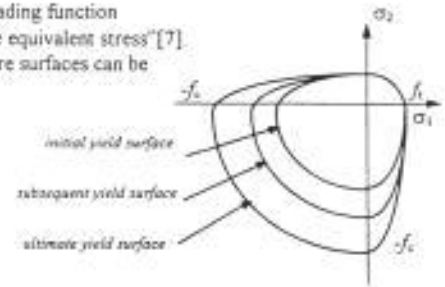

Fig.(1)- Yield surfaces of concrete in the two dimensional principal stress plane

$$[C]_c = \begin{bmatrix} 0 & 0 & 0 \\ 0 & E_t & 0 \\ 0 & 0 & \mu G_c \end{bmatrix} \;\&\; [C]_c = \begin{bmatrix} 0 & 0 & 0 \\ 0 & 0 & 0 \\ 0 & 0 & \mu G_c \end{bmatrix} \qquad (2)$$

While the incremental plastic stress-strain relations for concrete can be written as follows [7].

$$[C]_{ep} = [C]_e - ([I] - \{g\}\{g\}^t[C]_e)/(\{g\}^t[C]_e\{g\}^{-1}) \qquad (3)$$

in which; $\{g\}^t = (1/\sigma_e)\{\sigma_x - \sigma_y/2\ ,\ \sigma_y - \sigma_x/2\ ,\ 3\tau_{xy}\}$, & $[C]_e = E_c/(1-\nu^2)\begin{bmatrix} 1 & \nu & 0 \\ \nu & 1 & 0 \\ 0 & 0 & (1-\nu)/2 \end{bmatrix}$

The constitutive matrix for crushed concrete is Nil.

By summing the stiffness contribution of each layer together, the material stiffness matrix $[D]_c$ for the concrete section can be expressed as;

$$\begin{bmatrix} N \\ M \end{bmatrix} = [D]_c \cdot \begin{bmatrix} \epsilon_o \\ k \end{bmatrix} \qquad (4.a)$$

$$\begin{bmatrix} \{N\} \\ \{M\} \end{bmatrix} = \sum_{j=1}^{k} \begin{bmatrix} (Z_{jt} - Z_{jb})[C]_j & Z_j(Z_{jt} - Z_{jb})\cdot[C]_j \\ Z_j(Z_{jt} - Z_{jb})\cdot[C]_j & Z_j^2(Z_{jt} - Z_{jb})[C]_j \end{bmatrix} \begin{bmatrix} \{\epsilon_o\} \\ \{k\} \end{bmatrix} \qquad (4.b)$$

Where $[C]_j$ is the constitutive matrix for each layer in global coordinates

Z_j, Z_{jt}, Z_{jb} are the distances between the middle surface of the section and the mid-depth, top surface, and bottom surface of the jth layer as shown in Fig(2).

$\{N\}^t = \{N_x\ ,\ N_y\ ,\ N_{xy}\}$,
$\{M\}^t = \{M_x\ ,\ M_y\ ,\ M_{xy}\}$,
$\{\epsilon_o\}^t = \{\epsilon_{ox}\ ,\ \epsilon_{oy}\ ,\ \gamma_{oxy}\}$ &
$\{k\}^t = \{k_x\ ,\ k_y\ ,\ k_{xy}\}$

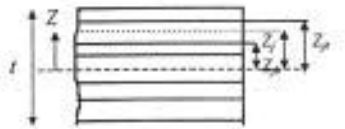

Fig.(2)- Layer notations of the section

Reinforcing Steel Layers

Reinforcing steel is treated as an equivalent uniaxial layered material placed at the depth of the center line of the bars and smeared out horizontally over the region of bars effect [7] as shown in Fig(3). The stress-strain curve of reinforcing steel is modeled by an idealized bilinear curve identical in tension and compression (see Fig. 4).

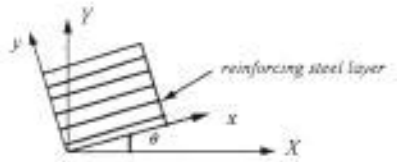

Fig (3)- Equivalent steel layer and material coordinates

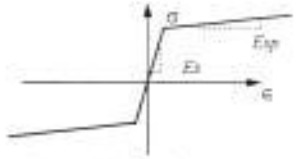

Fig.(4)- Idealized stress-strain curve for steel

The dowel action is neglected and the steel-concrete bond is assumed to be perfect. The constitutive matrices for steel layers in the material coordinate in both elastic and plastic regions, respectively, are:

$$[C]_e = \begin{bmatrix} \rho_s E_s & 0 & 0 \\ 0 & 0 & 0 \\ 0 & 0 & 0 \end{bmatrix} \quad \& \quad [C]_p = \begin{bmatrix} \rho_s E_{sp} & 0 & 0 \\ 0 & 0 & 0 \\ 0 & 0 & 0 \end{bmatrix} \tag{5}$$

The material stiffness matrix $[D]_s$ for reinforcing steel layers can be written as;

$$\begin{bmatrix} N \\ M \end{bmatrix} = [D]_s \begin{bmatrix} \epsilon_o \\ k \end{bmatrix} \tag{6.a}$$

$$\begin{bmatrix} \{N\} \\ \{M\} \end{bmatrix} = \sum_{j=1}^{k} \begin{bmatrix} 2.[C]_j & 2Z_j.[C]_j \\ 2Z_j.[C]_j & 2Z_j^2.[C]_j \end{bmatrix} \begin{bmatrix} \{\epsilon_o\} \\ \{k\} \end{bmatrix} \tag{6.b}$$

F.R.P Layers

FRP is treated as an equivalent biaxial layered material placed at the depth of center line of fibers and smeared out horizontally over the region of the FRP sheet effect [5] as shown in Fig(5). The stress-strain curve of the FRP sheet in the fiber direction is modeled by an idealized linear curve in tension as shown in Fig (6).

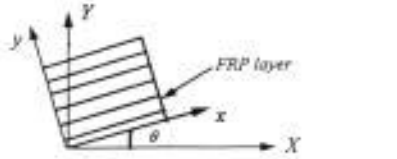

Fig(5)- Equivalent FRP layer and material coordinates for FRP

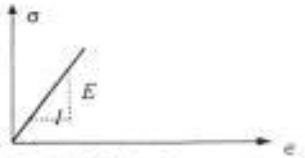

Fig.(6)- Idealized stress-strain curve for FRP

The incremental constitutive matrix for the FRP layer in the material coordinate, as shown in Fig(5), can be written as:

$$[C]_0 = \begin{bmatrix} Q_{11} & Q_{12} & 0 \\ Q_{21} & Q_{22} & 0 \\ 0 & 0 & Q_{12} \end{bmatrix} \tag{7}$$

where the items Q_{ij} are the coefficients of the stiffness matrix and are expressible in terms of the engineering elastic constants by,

$Q_{11}=E_{11}/(1-\nu_{12}\nu_{21})$, $Q_{22}=E_{22}/(1-\nu_{12}\nu_{21})$, $Q_{12}=Q_{21}=\nu_{21}E_{11}/(1-\nu_{12}\nu_{21})$ & $Q_{12}=G_{12}$ (8)

Similar to concrete and steel layers, the material stiffness matrix $[D]_f$ for the FRP layers can be expressed as;

$$\begin{bmatrix} N \\ M \end{bmatrix} = [D]_f \begin{bmatrix} \epsilon_o \\ k \end{bmatrix} \tag{9.a}$$

$$\begin{bmatrix} \{N\} \\ \{M\} \end{bmatrix} = \sum_{j=1}^{k} \begin{bmatrix} (Z_j - Z_{j-1}).[C]_j & Z_j(Z_j - Z_{j-1}).[C]_j \\ Z_j(Z_j - Z_{j-1}).[C]_j & Z_j^2(Z_j - Z_{j-1}).[C]_j \end{bmatrix} \begin{bmatrix} \{\epsilon_o\} \\ \{k\} \end{bmatrix} \tag{9.b}$$

DEVELOPMENT OF THE FINITE ELEMENT COMPUTER PROGRAM

The developed element model is a quadrilateral isoparametric 4-nodes element with five degrees of freedom (u , v , w , θ_x , θ_y) per node as shown in Fig(7). The generalized displacements: $\{\delta\}^t = \{u, v, w, \theta_x, \theta_y\}$ in each element can be represented by [8],

$$u=\sum_{i=1}^{n} h_i.u_i \ , \ v=\sum_{i=1}^{n} h_i.v_i \ , \ w=\sum_{i=1}^{n} h_i.w_i \ , \ \theta_x=\sum_{i=1}^{n} h_i.\theta_{xi} \text{ and } \theta_y=\sum_{i=1}^{n} h_i.\theta_{yi} \tag{10}$$

where $u_i, v_i, w_i, \theta_{xi}, \theta_{yi}$ are the nodal displacements for i^{th} node

h_i is the interpolation function at node i

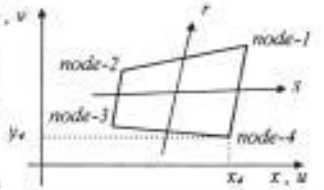

Fig.(7) Four node two-dimensional isoparametric element

In order to develop the element stiffness matrix [k], the material stiffness matrix [D] for the R.C section repaired by FRP is required to relate stresses {f} to strains {∈} in a way that,

$$\{f\} = [D] \ . \ \{\epsilon\} \tag{11}$$

where $[D] = [D]_c + [D]_s + [D]_f$

$\{f\}^t = \{ N_x , N_y , N_{xy} , M_x , M_y , M_{xy} \}$

$\{\epsilon\}^t = \{ \epsilon_{xo} , \epsilon_{yo} , \gamma_{xyo} , k_{xx} , k_{yy} , k_{xy} \}$ (12)

The strain-displacement relationship is given by;

$$\{\epsilon\} = [B].\{u\} \tag{13}$$

where {u} is a vector listing the element nodal point displacements and [B] is the strain-displacement transformation matrix.

The element stiffness matrix corresponding to the local element degrees of freedom is then :

$$[k] = \int_v [B]^T [D] [B] dv \qquad (14)$$

where v is the volume of the element.

To reflect the nonlinear behavior of reinforced concrete, as defined previously, the matrix [D] must be modified to accommodate the material models in the previous sections. The full details for modification of the matrix [D] is stated elsewhere [4].

By using the modified elastic procedures in an iterative manner, progressively refining the calculated material stiffness matrices [D] for each element, a nonlinear analysis can be carried out. The proposed algorithm of the nonlinear analysis procedure is summarized in the flow-chart shown in Fig.(8) and is described herein.

The structure properties (e.g. joint coordinates, element index, support coordinates, etc..) and material properties (e.g. concrete strength, reinforcement orientation, percentage and strength, element thickness, etc..) are firstly defined. Then, joint loads or distributed element loads are input and a nodal force vector {R} is calculated. Tangent stiffness values for the materials in each element are calculated and the material stiffness matrices [D] are computed. For the first iteration, the coefficients for an uncracked isotropic material can be used. The element stiffness matrices [k] for each element are calculated using Equation (14), and the overall structure stiffness matrix [K] is assembled. The matrix [K] is then inverted, and the unknown nodal point displacements {r} are obtained as follows,

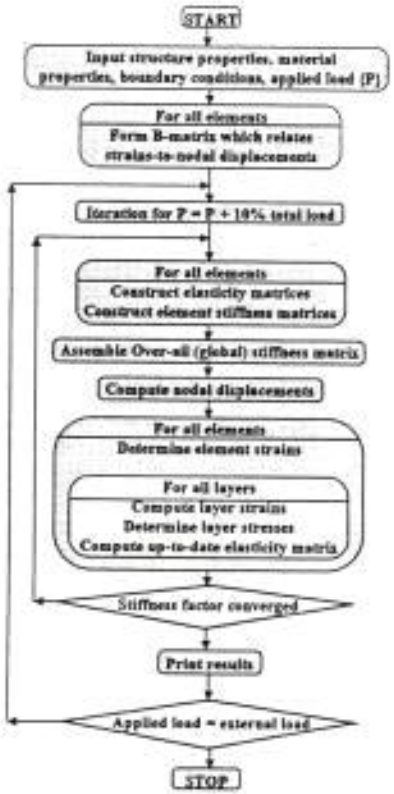

Fig (8)-General flow-chart of the computer program

$$\{r\} = [K]^{-1} . \{R\} \qquad (15)$$

The element strains and stresses can be determined by using back substitution of the nodal displacements into Equations (13), and (11) respectively

After determining the strains , new tangent moduli are then calculated for each element and a new material stiffness matrix [D] is calculated consequently for each element. If the material stiffness matrices have not converged, or in other words, if [D] ≠ [D], then [D] can be used as the new estimate and the analysis is repeated. After several iterations, the calculated values will converge and final results can be obtained [9].

NUMERICAL APPLICATIONS

Accuracy of The Program

In order to assess the accuracy of the developed computer program, three examples are presented. The first one is a square isotropic plate, P1, clamped along all four edges and loaded by a uniformly distributed load, q. Second example, P2, is a square isotropic plate with all edges simply supported and loaded by a transverse uniformly distributed load, q. The third example, P3, is a rectangular laminated composite plate made of Graphite-Epoxy with cross-ply (0/90) laminates. The plate is simply supported from all edges with length, a, to width, b, ratio of 2 (a/b = 2). The studied plates were divided into 4, 8, 16, and 64 elements as shown in Fig.(9), and the results obtained from the developed finite element program are compared to the results obtained from an exact solution [10,11] in Table (1). Excellent agreement is obtained between the 64 element solution and the exact one, and it is clear that the accuracy of the solution increases as the mesh is refined.

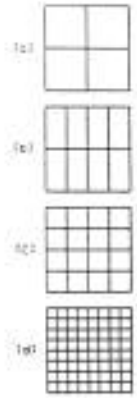

Fig (9)-Distribution of elements for studied plate case

Table-1 A comparison between the numerical results and the exact solution

Elements	*Mesh*	*transverse deflection*		
		P1	P2	P3 (0/90)
4	2×2	0.001468	0.003431	1.857665
8	2×4	0.001428	0.003647	2.100784
16	4×4	0.001393	0.003921	2.302657
64	8×8	0.001300	0.004028	2.337658
Exact solution[10,11]	.....	0.001260	0.004060	2.349000
Multiplier	.....	$q\ a^4/D$	$q\ a^4/D$	$E_{22}\ t^3/q\ b^4.100$

D	$E\ t^3/12\ (1-\nu^2)$
E	Young's modulus
E_{11},E_{22}	modulus of elasticity in long and short directions
t	thickness of the plate
ν	Poisson's ratio

Nonlinear Analysis of R.C Plates

Two numerical examples are presented in order to evaluate the capability of the developed computer program to represent the nonlinear behavior of reinforced concrete plates. These examples include square and rectangular reinforced concrete plates. A comparison between the numerical and experimental or theoretical results is also provided.

Simply supported R.C square plate

The reinforced concrete square plate (250× 250× 10cm), tested elsewhere [10], is modeled using the developed finite element program into sixteen elements per quarter of the plate because of the double symmetry. The plate is subjected to a uniformly increasing load upto 120 kPa and is reinforced by 8×8cm spacing wire mesh of diameter 8mm while top reinforcement was placed in corners.

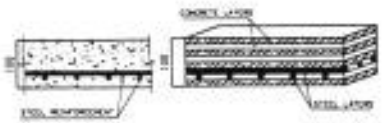

Fig (10)- Cross-section and layered model of the simply supported plate

The R.C section and layered model of the plate are shown in Fig.(10). The uniaxial compressive and tensile strength of concrete were 33.5Mpa (341.7Kg/cm^2) and 3Mpa (30.6Kg/cm^2), respectively. The initial modulus of elasticity was 3400Mpa (346800 Kg/cm^2), the yield stress of steel was 500Mpa (5100Kg/cm^2) and the concrete cover was 1cm. The static response of the plate was predicted by the developed program and compared with the experimental and theoretical results reported in [10]. Fig.(11) shows that the numerical results provide a reasonably accurate simulation of the test panel behavior. It is worth mentioning that the nonlinear analysis results differ substantially from the results of linear elastic uncracked material model (see Fig. 11).

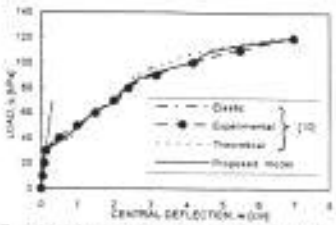

Fig.(11)- Load-deflection curves for simply supported square plate

Simply supported R.C rectangular plate

A simply supported rectangular plate (200×300×8cm), experimentally tested by Franz [10] and analytically solved by Link and Lewinski [10], is reanalyzed using the proposed model in order to assess its accuracy. The plate was loaded by a uniformly distributed load, and reinforced by 9×20cm spacing wire mesh of diameter 8mm. The plate properties, dimensions, and finite element mesh are shown in Fig(12).

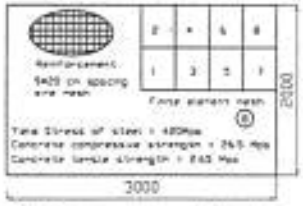

Fig.(12) Plate properties and finite element mesh of the rectangular plate

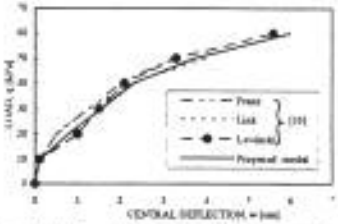

Fig.(13)- Load deflection curves for simply supported rectangular plate

The numerical results obtained by the proposed model were compared with the experimental and theoretical results reported in [10]. Excellent agreement was found between the results obtained by the numerical model and the results reported in [10] as shown in Fig(13).

The crack pattern, of the plate was predicted by the developed finite element model for loading level of 40 kPa. It can be seen from Fig(14), that there is a good agreement between the predicted crack pattern and the one obtained experimentally in [10].

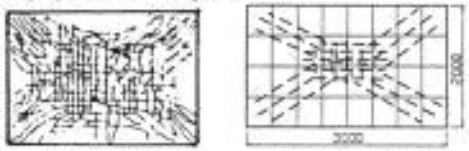

Experimental crack pattern *Predicted crack pattern*

Fig.(14)- Crack patterns for numerical and experimental results

Retrofitting of R.C. Plates With FRP

Since there is limited information in the literature about the experimental and theoretical behavior of R.C slabs retrofitted using FRP, the study in this section shall be based only on the nonlinear analysis using the developed computer program.

The simply supported rectangular R.C plate (200×300×8cm), analyzed in the previous section, is considered to be strengthened by a one layer of FRP sheet of thickness 3mm attached to its bottom surface (tension zone) using a suitable adhesive material. The data supplied by the manufacturer for the FRP material are as follows: the maximum tensile strength is 2.8Gpa (28620Kg/cm^2), E_{11} is 165Gpa (1700000Kg/cm^2), E_{22} is 1.65Mpa (17000Kg/cm^2), and Poisson's ratio is 0.3. Different fiber orientations for the FRP sheet, (0,30,45,60,90°), are considered in the analysis in order to study their effect on the behavior of the plate. The deflection values at load = 40 kPa for R.C slab before and after attaching FRP sheets to the bottom surface are shown in Fig(15). It can be seen from the figure that using FRP sheet of one layer (thickness = 3mm) reduces the center deflection value by about 40%. It is also clear from Fig(15) that the minimum deflection is obtained by attaching the FRP sheet of 90° fibers orientation angle. This is probably because the sheet of this orientation works as a reinforcement in the short direction of the studied plate.

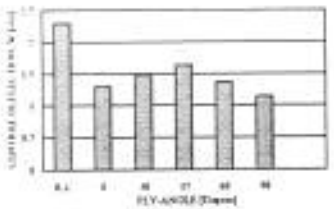

Fig.(15)- Deflection values for R.C slab repaired by FRP sheets of different fibers orintation

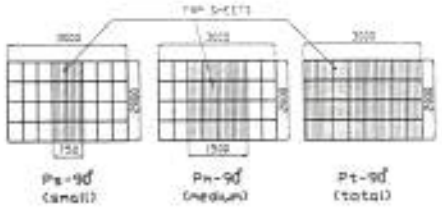

Fig.(16)- Strengthening R.C slab with FRP sheets of different sizes

In order to study the behavior of plates partially retrofitted by FRP, three plate cases strengthened by FRP sheets of different sizes but with the same properties as defined previously and fibers orientation of 90° are analyzed. The configuration and dimensions of the attached FRP sheets are shown in Fig(16). A comparison between the over all load-deflection curves for the plates strengthened with different sizes of FRP sheets and the control R.C plate is shown in Fig(17).

Complete strengthening with FRP sheet (Pt-90) resulted in a significant reduction in deflection for different loading levels. However, such complete strengthening is rarely recommended in practice for economic reasons and in fact it is seldom structurally justified. On the other hand, strengthening with FRP sheet of small size (Ps-90) is likely to lead to cracking which may be unacceptable for special structures. It may be argued that the retrofitting with FRP sheet of medium size (Pm-90) is the best structural solution in the cases studied herein.

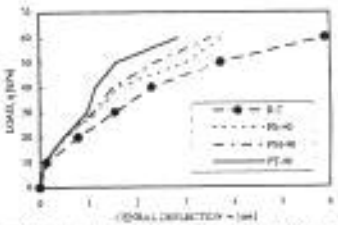

Fig.(17)- Load-deflection curves for different sizes of attached FRP sheets

CONCLUSIONS

The good agreement between the numerical and experimental results established the validity and accuracy of the proposed material model and developed nonlinear finite element program for predicting the flexural behavior of R.C plates and those strengthened by FRP sheets. The proposed material modeling can be easily programmed into any finite element package.

Within the scope of the current investigation, retrofitting R.C plates using FRP sheets reduced the center deflection by about 40%. This was more pronounced where the fiber orientation angle was perpendicular to the major crack directions.

It is recommended that the partial retrofitting with FRP is employed for economic and structural reasons.

REFERENCES

1. Saadatmanesh H. , *"Fiber composites for new and existing structures "*; ACI Structural Journal, May-June, 1994, pp. 346-354.
2. Amir Z. Fam, Sami H. Rizkalla, and G. Tadros," *Behavior of CFRP for prestressing and shear reinforcements of concrete Highway Bridges*", ACI Structural Journal, Vol.94, No. 1, Jan-Feb. 1997.
3. Hoskin, C. B., and Baker, A. A., *"Composite material for aircraft structures "*; AIAA Education series, American institute of aeronautics and Astronautics, Inc., New York, 1986.
4. Wael Abo Elmagd, *"Retrofitting of tow-way reinforced concrete slabs using advanced composite materials"*, Master of engineering Science thesis (in preparation), Zagazig university, Banha branch, Shoubra, Egypt.
5. Ibrahim I.M. , and Shaaban I.G., *"Analysis and behavior of FRP composites for new and existing structures "*, The first Middle East Workshop on advanced composite materials, Sharm El shaik, Egypt, June-1996.
6. Chen W. F., *"Plasticity in reinforced concrete"*; McGraw-Hill Book Company, Inc., 1982.
7. Hu H.-T. and Schnobrich W. C., *"Nonlinear finite element analysis of reinforced concrete plates and shells under monotonic loading"*; Computers & Structures, Vol.38, No. 5/6, pp. 637-651, 1991.
8. Singh G., and Sadasive Rao Y. V. K., *"Stability of thick angle-ply composite plates"*; Computers & Structures, Vol. 29, No. 2, PP. 317-422, 1988.
9. Vecchio F. J., *"Nonlinear finite element analysis of reinforced concrete membranes"*; ACI Structural Journal, Jan. 1989, PP. 26-35.
10. Lewinski P. M., and Wojewodzki W., *"Integrated finite element model for reinforced concrete slabs"*; Journal of Structural Engineering, Vol. 117, No. 4, April, 1991.
11. Danielson K. P., and Tielking J. T., *"Membrane boundary condition effects on unsymmetric laminates"*; Journal of Engineering Mechanics, Vol.114, No. 12, Dec. 1988.

NOTATION

E_s , E_p	elastic, and plastic modules for steel.
E_{11} , E_{22}	longitudinal, and transverse modules for FRP.
E_o , E_t	initial, and tangent modulus for concrete.
G , G_c	shear moduli of uncracked and cracked concrete respectively.
ν	Poisson's ratio of concrete.
ν_{12} , ν_{21}	Poisson's ratio in longitudinal and transverse directions for FRP layers.
σ_x , σ_y	stresses of concrete in x , y directions.
σ_o	the yield stress of concrete in uniaxial compression.
τ_{xy}	shear stress for concrete.
μ	shear retention factor.
ρ_i	steel percentage for the ith layer.
f_c , f_t	maximum compressive strength and maximum tensile strength of concrete
$[C]_c$	routing crack tangent constitutive matrix for concrete.
$[C]_e$, $[C]_{ep}$	elastic, and elastoplastic material matrices respectively
$[C]_{si}$	constitutive matrix for the ith steel layer in material coordinates.
$[C]_{fi}$	constitutive matrix for the ith FRP layer in material coordinates.
{f}	element stress vector.
{g}	plastic potential function
{I}	unit matrix
{k}	vector of middle surface curvatures.
{N} , {M}	vectors of stress an moment resultants.
{ε}	strain vector in global coordinates.
$\{\varepsilon_o\}$	vector of middle surface strain.

Proceedings of the Seventh Arab Structural Engineering Conference
24 - 26 November 1997 Kuwait

الأبنية العالية ذات النواة الصلبة المقاومة للزلازل

د. م. ميادة الأحمد الكوسا – جامعة دمشق – كلية الهندسة المدنية

الملخص :

يطرح البحث إقتراح حل إنشائي جديد للأبنية العالية المقاومة للزلازل ذات الجملة الإنشائية المشتركة للنواة الصلبة والإطارات وذلك بجعل العقد الواصلة بين الإطارات والنواة الصلبة بشكل مفاصل، وتمت دراسة تأثير هذا الشكل للإتصال على قيمة القوى الاقفية الناتجة عن تأثير الزلازل وعلى الصفات الديناميكية للمنشأ حيث تبين أن هذا الحل يخفض من قيمة القوى القاصة وبالتالي من قيم التسليح اللازم للأعمدة والجوائز ويزيد من مدة الدور الذاتي للإهتزاز.

ABSTRACT:

This research presents an innovative technique for seismic resisting high - rise shear wall - frame building.

The proposed technique uses pin - ended beams as connecting members between rigid core and framing systems. The effects of pin-ended connectors on the value of seismic horizontal shear forces and the dynamic properties of the building were fully investigated.

Obtained results indicate that the proposed type of connections reduce the value of base shear and increase the value of the fundamental period of the building . These later two effects reduce drastically the amount of needed reinforcements for both beam and column systems of the building